

Photographic observation of a natural fourth-order rainbow

Michael Theusner

Klinthöfe 10, 27619 Schiffdorf, Germany (michael@theusner.eu)

Received 10 August 2011; revised 29 August 2011; accepted 29 August 2011;
posted 30 August 2011 (Doc. ID 152688); published 30 September 2011

We report what is believed to be the first photographic recording of a quaternary rainbow in nature. It appears on the Sun side of the sky with its red arc at a radius of about 45° from the Sun. The original pictures have been subjected to various forms of image processing to reveal the tertiary rainbow as well as the quaternary rainbow, which are separated by only a few degrees with their colors reversed and their red arcs adjacent to each other. © 2011 Optical Society of America
OCIS codes: 010.1290, 010.1310, 010.3920, 010.7295, 290.4020.

1. Introduction

Rainbows are a phenomenon often observed in nature. The most common rainbows are the primary and secondary rainbow (first- and second-order rainbow), which are caused by sunlight suffering one or two internal reflections respectively within rain drops [1]. These rainbows appear as circular arcs at angular distances of 40° – 42° and 50° – 53° , respectively, around the antisolar point.

Theoretically, higher order rainbows exist as well, but there are very few reports of visual sightings of higher order bows in the literature [2]. These reports are all limited to the third-order rainbow. There are several reasons why higher order rainbows are rarely, or not at all, visible. Firstly, each additional reflection results in a loss of intensity. Furthermore, with each reflection, the angular dispersion of the rainbow increases and, hence, its angular width increases. Therefore, the intrinsic brightness of higher order bows is much less than that of the primary and secondary rainbows. For the third-order bow, the brightness is 0.24 of that of the primary bow, and this value drops to 0.15 for the fourth-order bow [1]. Another, and even more important, factor that affects the visibility is that the tertiary and quaternary bows form on the sunward side of the sky at about 38° – 42° and 44° – 48° around the Sun. This is well within the area of the bright zero-order glow—the

part of the sky that is lit by sunlight passing through rain drops without any internal reflection. This unfortunate position accounts for the very low contrast between the already faint third- and fourth-order bows and the background, explaining the small number of visual observations of the former and the apparent absence of any report of the latter. According to Lee and Laven [2], seeing with the naked eye the third-order bow may just be possible under exceptional lighting conditions with brightly lit rain and a dark sky background (dark clouds).

Under such conditions, Großmann *et al.* [3] has reported a visual observation of the third-order bow on May 15, 2011, in conjunction with its first photographic evidence using a standard consumer digital camera (DSLR). A preliminary report of this observation [4] (see [5] for an English version) posted in the Internet discussion forum of the Arbeitskreis Meteore e.V., the German association for the observation of atmospheric phenomena, inspired the author to try to detect the third-order rainbow using a technique that is well known in astrophotography: several images are “stacked” (or superimposed) so as to improve the signal-to-noise ratio in digital camera images. This technique enabled the chance discovery of the fourth-order rainbow described here.

2. Observation

On the evening of June 11, 2011, a large area of heavy convective precipitation approached from the southwest the author’s hometown Schiffdorf near Bremerhaven in Northern Germany. Behind that

area, mostly clear skies prevailed and provided for a perfect setting to observe rainbows. Heavy precipitation reached the observing site (a field road north of Schiffdorf; 53.55°N, 8.65°E) at about 18:00 UTC. While rain was still falling, the Sun came out at 18:13 UTC, but was still partially covered by clouds. The clouds moved toward the northeast, covering the sky from the northwest to the south-southwest and above 12° altitude. The Sun in the west-northwest and the dark clouds in the north created the situation conducive for the observation of the third-order rainbow described by [2,3].

As soon as the Sun came out, a series of five images was taken in continuous mode, which typically takes less than 1 s. This was repeated approximately every minute. The camera was pointed at the dark clouds in the direction of where the third-order bow was expected to form (i.e., about 40° to the right of the Sun). At that time, a weak primary rainbow was visible in the opposite part of the sky.

After 18:17 UTC the Sun was free of clouds and the raindrops were brightly lit. A bright primary and a secondary rainbow formed. The rain stopped at the observing site at approximately 18:24 UTC and no further images were taken in the direction of the third-order rainbow. In total, nine series of five images each were collected during the observation. In that time span, the solar altitude had dropped from 11.2° on 18:17 UTC to 10.2° on 18:24 UTC (solar altitude data from USNO [6]).

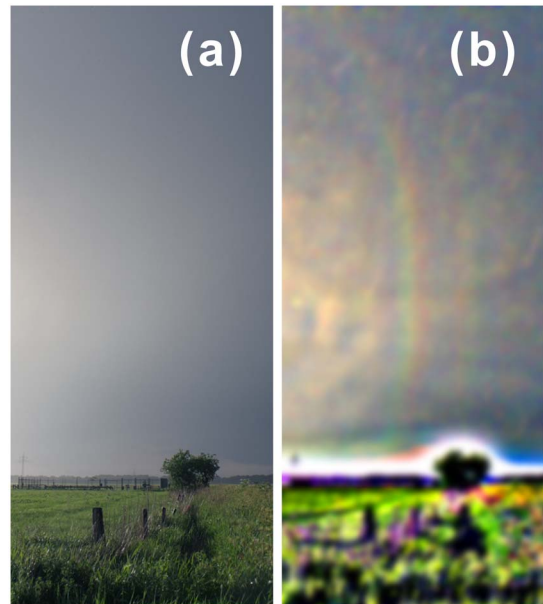


Fig. 1. (Color online) (a) The stacked image (cropped) generated from the image series of June 11, 2011, 18:19 UTC. (b) Processed version (unsharp masking, increased saturation, Gaussian smoothing), which shows two rainbow-like arcs with reversed colors.

Neither the third- nor the fourth-order rainbow was seen visually during the observation and they are also not apparent in the original, unenhanced images.

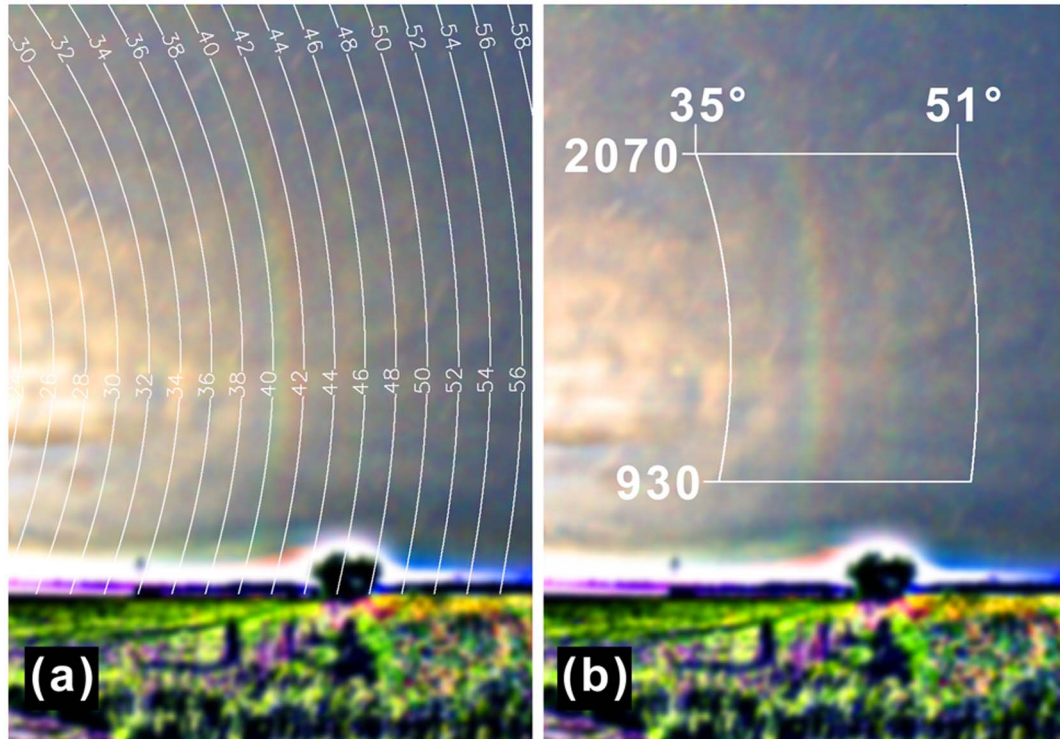


Fig. 2. (Color online) (a) Distance in degrees of the pixels from the location of the Sun as computed from the astrometric solution and compensating for lens distortion. The circles trace the shapes of the tertiary and quaternary rainbows. (b) Area of the image where pixels were averaged along each Sun-centered circle at 0.05° increments. Pixel rows 930 to 2070, and Sun-centered radii between 35° and 51° were used.

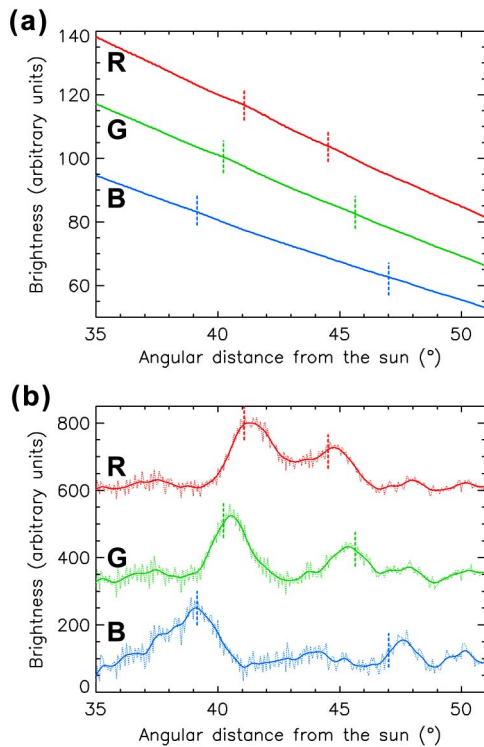


Fig. 3. (Color online) Brightness data of the RGB channels (top to bottom, respectively) of the stacked image (Fig. 1) for the area highlighted in Fig. 2(b). (a) Original data. (b) Individual polynomial subtracted. The two dashed vertical lines in each graph mark, for the centroid wavelength of the channel, the positions of the third- and fourth-order rainbow angles as given in Table 1.

The camera used was a Canon 40D with an EF-S 17–55 mm lens set to 17 mm focal length (equivalent to a focal length of about 27 mm for a 35 mm film camera). All images were taken in RAW mode at full resolution (3888×2592 pixels) and picture style “neutral.” The camera’s clock was calibrated before and after the images were taken. The difference was 1 s when the second calibration was performed.

The RAW images were converted to 16 bit TIFF files using Canon’s Digital Photo Professional software. No additional processing functions were applied to the images in this step. The images of each series were then stacked, resulting in nine stacked images. Neither the third- nor the fourth-order rainbow is apparent in any of the unprocessed stacked images [Fig. 1(a)].

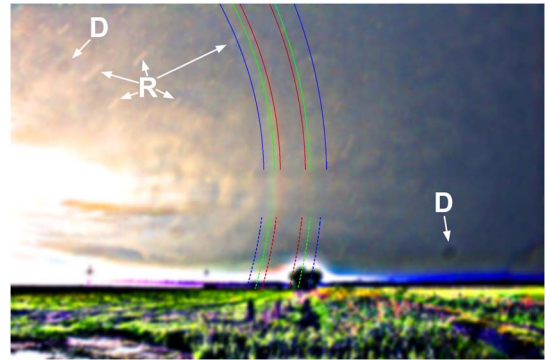


Fig. 4. (Color online) Measured (solid lines) and modeled (centroid wavelengths; dashed lines) radii of the third- and fourth-order rainbows. Some dust specks (*D*) and trails of sunlit raindrops (*R*) are marked.

These images were then further processed. Increasing saturation and applying unsharp masking and smoothing to the images revealed that a third-order rainbow was recorded in all the images taken from 18:17 UTC, i.e., the time when the clouds had moved away from the Sun sufficiently so that the raindrops were brightly lit. In the image series taken at 18:19 UTC the third-order bow is clearly visible in each of the single images after processing and a segment of the fourth-order rainbow in the stacked image [Fig. 1(b)]. The characteristics of the bows are just as described by [7]: reverse sequence of colors with the red sides facing each other.

3. Analysis

A. Referencing

Determining the radii of the rainbows detected in the processed images allows comparison with the expected values from the literature. In that way it can be checked whether or not these bows are indeed the third- and fourth-order rainbow.

Several steps had to be performed: (1) Relate the pixels of an image to equatorial coordinates (right ascension and declination) using the location of stars. (2) Determine the celestial location of the Sun from the known time the images were taken. (3) Compute the distance in degrees between a pixel and the location of the Sun along the great circle connecting the two points. (4) Stack the pixel values along circles centered on the Sun to create a data set that relates

Table 1. Measured and Predicted Radii for the Peak and Centroid Wavelengths of the RGB Channels

Rainbow	Sensor Channel	Measured Radius	Radius After [10]	
			Peak Wavelength ^a	Centroid Wavelength ^a
3rd order	R	41.35°	41.03° (−0.32°)	41.09° (−0.26°)
	G	40.55°	40.09° (−0.46°)	40.23° (−0.32°)
	B	39.10°	38.71° (−0.39°)	39.15° (+0.05°)
4th order	R	44.75°	44.60° (−0.15°)	44.53° (−0.22°)
	G	45.35°	45.50° (+0.15°)	45.64° (+0.29°)
	B	47.60°	47.59° (−0.01°)	47.02° (−0.58°)

^aThe deviations of the predicted from the observed locations of the radii are given in parentheses.



Fig. 5. (Color online) Composite image made by using different masks to retain the natural look of the foreground while still showing the contrast-enhanced tertiary and quaternary rainbows in the sky. The white streaks are individual raindrops.

pixel brightness to radius. This is done for each of the three channels of an image (R, G, and B).

To achieve step 1, a reference image at the observing location was taken at night on June 30, 2011. Ideally, this image should show the same field of view as the rainbow images. Objects (electricity poles, trees) at a distance of several kilometers were used to carefully align the camera. In the end the maximum deviation between the two fields of view was five pixels, which corresponds to an uncertainty of about 0.1° .

The stars in the image then allow the equatorial coordinates to be deduced for each pixel of the image. First, a preliminary astrometric solution is computed for the image from the pixel coordinates and celestial coordinates of three stars in the field of view. This was done using the *starast.pro* program from NASA's IDL astronomy library [8]. This astrometric solution was then corrected for lens distortion. To achieve that, stars were marked over the whole field of view. Their pixel locations in the image were then compared to the ones computed from the preliminary astrometric solution (using the celestial coordinates of the stars). From these two data sets, the parameters of a fourth-order polynomial were computed. This polynomial can then be employed to warp the pixel coordinates such that application of the preliminary astrometric solution yields the correct equatorial coordinates. Comparing the actual and computed equatorial coordinates of the stars shows that this method is accurate to about 0.01° .

From the computed celestial coordinates of each pixel and those of the Sun, the distances in degrees

of the pixels from the Sun were derived using the respective trigonometric functions (step 2 and 3).

B. Rainbow Analysis

Stacking the pixel values for each radius was done at 0.05° intervals for each of the three channels of the image. Radii between 34° and 51° were analyzed, covering the range where the third- and fourth-order rainbows occur. Vertically, the section where both rainbows are visible was used ($y = 930$ to $y = 2070$; see Fig. 2).

The results are displayed in Fig. 3(a). A strong brightness gradient is evident that is due to the zero-order glow. To extract the signal of the rainbows, this gradient was removed using individual polynomials for each of the three color channels [Fig. 3(b)]. These polynomials were fitted to radius values omitting those of the bows. The radius values for the two bows are listed in Table 1 and displayed in Fig. 4.

The conversion of RGB values to wavelengths requires knowledge of the spectral response of the camera's sensor. The peak and centroid wavelengths were computed from publicly available data [9] (the centroid wavelength is the geometric center of the sensor's response function). This indicates that the RGB sensors correspond approximately to wavelengths of 600 nm, 530 nm, and 486 nm (centroid) and 595 nm, 521 nm, and 448 nm (peak), respectively.

Table 1 shows a comparison of the observed radii of the bows with the values modeled by use of Debye series calculations [10]. It confirms that the image does, indeed, show the third- and fourth-order rainbows and thus provides the first photographic

evidence of the fourth-order bow. However, there are some discrepancies between the locations of the modeled, measured, and visually apparent colors of the quaternary bow. These may be due to several factors. Artifacts from the structure of the clouds, raindrops (bright streaks and spots), and dust specks on the sensor (dark spots), which are all readily visible in the image (Fig. 4), may distort the measured radii. These artifacts will have a larger impact on the fainter quaternary bow than on the brighter tertiary. Additionally, errors may have been introduced during the referencing process leading to mismatches. Furthermore, the size of the water drops has a significant effect on the radii of the bows [11].

4. Summary and Recommendations

This paper presents the first photographic documentation of a natural quaternary rainbow. The images also represent the second photographic documentation of a natural tertiary rainbow, just one month after its first recording by Großmann *et al.* [3]. Despite the very low contrast between the zero-order glow and the third- and especially the fourth-order rainbows it proves to be possible to photograph these higher order bows and to identify their nature. The observation quantitatively confirms the general belief (see [2]) that detection of these rainbows requires some exceptional circumstances such as those encountered here. We conclude that a good strategy for detecting is to collect several images in short succession in order to enable stacking and thus for a better signal-to-background ratio. As higher order rainbows are strongly polarized ($>75\%$), the use of a polarizer could increase the signal-to-background ratio by almost a factor two [12].

The following recommendations are given for future attempts:

1. Shield the camera from rain to prevent raindrops on the lens (and damage to the camera).
2. Use a stable tripod to ensure a fixed field of view.
3. Measure the camera's height above the ground and record the location of the tripod by taking a photo

(allows to quickly find the correct field of view for the star field image).

4. Record as many images as possible in a burst lasting a few seconds.
5. Use RAW format to allow 16 bit-processing.
6. Record a star field with the same field of view at night to enable referencing the coordinate system of the image.
7. The use of a polarizer may help to improve the signal-to-background ratio of the tertiary and quaternary rainbows.

Figure 5 summarizes the observations with a composite image showing the tertiary and quaternary rainbow above the unenhanced foreground.

The author thanks Gunther Können and Philip Laven for their advice and support.

References

1. M. Vollmer, *Lichtspiele in der Luft* (Spektrum Akademischer Verlag, 2006).
2. R. L. Lee, Jr., and P. Laven, "Visibility of natural tertiary rainbows," *Appl. Opt.* **50**, F152–F161 (2011).
3. M. Großmann, E. Schmidt, and A. Hausmann, "Photographic evidence for the third order rainbow," *Appl. Opt.* **50**, F134–F141 (2011).
4. M. Großmann, "Regenbogen 3. Ordnung 15.05.2011," <http://www.meteoros.de/php/viewtopic.php?t=8463>.
5. M. Großmann, "Natural tertiary rainbow 3rd order," <http://atoptics.wordpress.com/2011/06/01/rainbow-3th-order-3/>.
6. USNO, "Data services—Naval Oceanography Portal," <http://www.usno.navy.mil/USNO/astronomical-applications/data-services>.
7. R. L. Lee, Jr., and A. B. Fraser, *The Rainbow Bridge: Rainbows in Art, Myth, and Science* (Pennsylvania State University, 2001).
8. W. Landsman, "The IDL Astronomy User's Library," <http://idlastro.gsfc.nasa.gov/contents.html>.
9. C. Buil, "Canon 40D, 50D, 5D, 5D Mark II Comparison," <http://astrosurf.com/buil/50d/test.htm>.
10. P. Laven, "MiePlot (v4.2)," <http://www.philiplaven.com/mieplot.htm>.
11. R. L. Lee, "Mie theory, Airy theory, and the natural rainbow," *Appl. Opt.* **37**, 1506–1519 (1998).
12. G. P. Können, Sophialaan 4, NL-3761DK Soest, The Netherlands (personal communication, August 2011).